DOI 10.1007/s11595-017-1563-4

Physical Properties of Al-doped ZnO and Ga-doped ZnO Thin Films Prepared by Direct Current Sputtering at Room Temperature

ZHU Ke[1], YANG Ye[2], LI Jia[2], SONG Weijie[2]

(1. Department of Physics and Mathematics, Hunan Institute of Technology, Hengyang 421002, China; 2. Ningbo Institute of Materials Technology and Engineering, Chinese Academy of Sciences, Ningbo 315201, China)

Abstract: Al-doped zinc oxide (AZO) and Ga-doped zinc oxide (GZO) thin films with the same doping concentration (3.6 at%) were deposited on glass substrates at room temperature by direct current (DC) magnetron sputtering. Consequently, we comparatively studied the doped thin films on the basis of their structural, morphological, electrical, and optical properties for optoelectronic applications. Both thin films exhibited excellent optical properties with more than 85% transmission in the visible range. The GZO thin film had better crystallinity and smoother surface morphology than the AZO thin film. The conductivity of the GZO thin film was improved compared to that of the AZO thin film: the resistivity decreased from 1.01×10^{-3} to 3.5×10^{-4} Ω cm, which was mostly due to the increase of the carrier concentration from 6.5×10^{20} to 1.46×10^{21} cm^{-3}. These results revealed that the GZO thin film had higher quality than the AZO thin film with the same doping concentration for optoelectronic applications.

Key words: room temperature; ZnO; thin films; sputtering; electrical properties

1 Introduction

Functional oxide materials have been widely applied to develop the next generation of transparent electronics, such as field-effect transistors, solid state sensors, solar cell and electrochromic devices[1,2]. As one of the most promising functional oxide materials, ZnO has been used as electrodes in optoelectronic devices, because of its excellent optoelectronic properties, non-toxicity, low material cost, and stability in hydrogen plasma processes[3-7]. Recently, the deposition of highly conductive Al-doped ZnO (AZO) and Ga-doped ZnO (GZO) thin films at low substrate temperature has received an amount of attention, since the low substrate temperature minimizes the interdiffusion processes on previously deposited materials and benefits the deposition of films on polymer substrates for flexible electronic device applications[8-10]. Compared with other techniques, direct current (DC) magnetron sputtering technique is used most often as it can prepare films on large areas at low deposition temperature, with good adhesion to the substrate, high deposition rate, and reproducibility[11-13]. Many researchers have employed DC magnetron sputtering technique to prepare highly conductive AZO and GZO thin films at low substrate temperature[11-15]. Tao *et al* reported the GZO thin films deposited on PEN substrate at room temperature with a resistivity as low as 6.65×10^{-4} Ω cm[13]. Pei *et al* reported the AZO thin films deposited on Al_2O_3-buffered PET substrate at room temperature with a resistivity of 8.4×10^{-4} Ω cm[14]. However, few studies have been reported on the comparison of the properties of AZO and GZO thin films prepared under the same doping concentration and deposition conditions.

In this paper, AZO and GZO thin films with the same doping concentration (3.6 at%) were deposited on glass by DC magnetron sputtering at room temperature. The structural, morphological, electrical and optical properties of the AZO and GZO thin films were compared in detail.

2 Experimental

AZO and GZO thin films were deposited on glass substrates from home-made 3.6 at% AZO (ZnO/Al_2O_3=96.4/1.8 at%) and GZO (ZnO/Ga_2O_3=96.4/1.8 at%) ceramic targets, respectively. Prior to deposition,

(Received: Oct. 20, 2015; Accepted: Nov. 4, 2016)

ZHU Ke(朱科) : Ph D; E-mail: xuezhouzk@163.com

Funded by National Natural Science Foundation of China(NSFC) (Nos.21205127, 61275114)

the substrates were sequentially cleaned in an ultrasonic bath with acetone, ethanol, and de-ionized water, and then blown dried with nitrogen gas. The distance between the target and substrate was fixed at 90 mm. The base pressure in the chamber was kept below 5 $\times 10^{-4}$ Pa. During the process of deposition, the film was grown at room temperature (about 25 ℃) for 15 min with the flow rate of Ar of 30 sccm, the deposition pressure of 0.4 Pa and the DC sputtering power of 200 W.

The phase structure of the thin films was analyzed by X-ray diffraction (XRD) with Cu Kα radiation in θ-2θ Bragg-Brentano geometry (Bruker, AXSD8 Advance, USA). The chemical structure and composition of the thin films were studied by X-ray photoelectron spectroscopy (XPS, Kratos AXIS ULTRADLD, UK). The XPS measurements were done after 30 s of Ar sputtering, in order to eliminate contaminants captured from the air. The thickness of the thin films was determined by a surface profilometer (Veeco, Dektak150, USA). The surface morphology was examined using an atomic force microscope (AFM, CSPM5500, China). The optical transmittance and reflection of the thin films were measured using an UV/VIS/NIR spectrophotometer (Perkin-Elmer, Lambda 950, USA). The resistivity, carrier concentration and mobility of the thin films were measured using Van der Pauw method by Hall measurements (Accent, HL5500PC, UK).

3 Results and discussion

The crystal structures of the AZO and GZO thin films were analyzed by XRD. The XRD patterns revealed strong preferred orientation (002) peaks as shown in Fig.1, indicating that the thin films were orientated with their axes perpendicular to the substrate plane. The (002) diffraction peak position of 34.31° for GZO thin film was relatively higher than that of 34.02° for AZO thin film, which could be due to the smaller difference in radius between Ga^{3+} ions (0.062 nm) and Zn^{2+} ions (0.074 nm) than with Al^{3+} ions (0.054 nm) and Zn^{2+} ions[16,17]. The GZO thin film showed stronger and sharper (002) diffraction peak than the AZO thin film. The average grain size calculated according to the Scherrer equation for the GZO thin film was 25.7 nm, larger than that of 22.8 nm for the AZO thin film. These results indicated the better crystal quality of the GZO thin film than that of the AZO thin film.

The chemical bonding configurations of AZO and GZO thin films were investigated by X-ray photoelectron spectroscopy (XPS). Fig.2 shows the curve-fit results of O 1*s* XPS spectra for the AZO and GZO thin films. The low binding energy component (denoted as OI) centered at 530.1 ± 0.1 eV is assigned to the lattice oxygen of ZnO[18,19]. The high binding energy component (denoted as OII) centered at 531.6 ± 0.1 eV is attributed to O^{2-} ions in the oxygen deficient regions within the matrix of ZnO[18,19]. The relative changes in the low and high binding energy components therefore reveal the degree of O-Zn bonding and oxygen vacancies. As shown in Fig.2, comparing to the AZO thin film, the level of O-Zn decreased and the level of oxygen vacancies increased for the GZO thin film. The increase of oxygen vacancies could contribute to the increase of the carrier concentration.

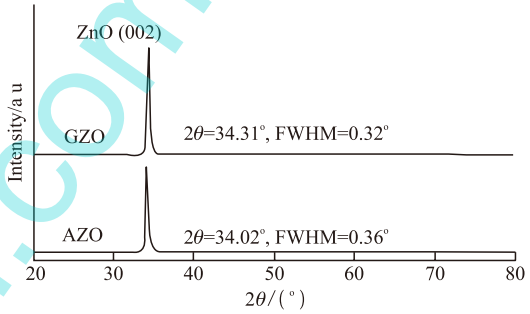

Fig.1 XRD patterns of the AZO and GZO thin films

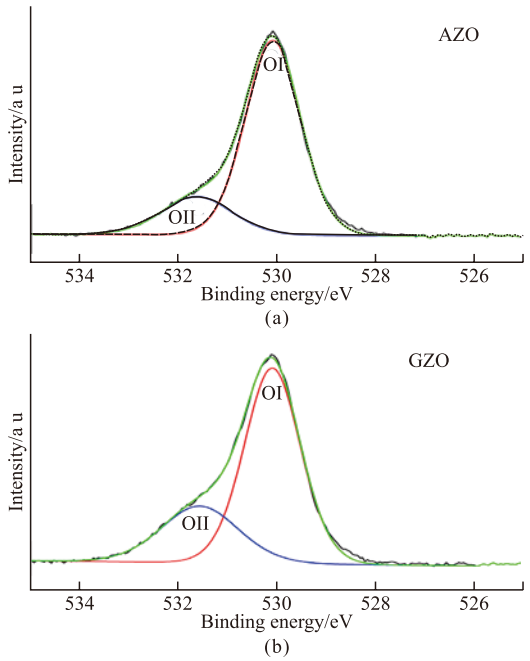

Fig.2 Curve-fit results of O 1*s* XPS peaks of the (a) AZO and (b) GZO thin films

The AFM images of the AZO and GZO thin films are shown in Fig.3. Both the AZO and GZO thin films exhibited similar dense and uniform morphology. The

GZO thin film showed a smoother surface morphology with the RMS roughness of 3.6 nm than the AZO thin film with the RMS roughness of 5.6 nm. The decrease in surface roughness reduced the absorption of oxygen and thus contributed to improving the electrical properties[20,21].

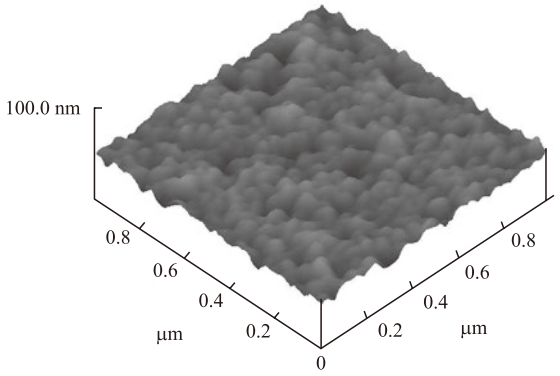

AZO RMS=5.6 nm
(a)

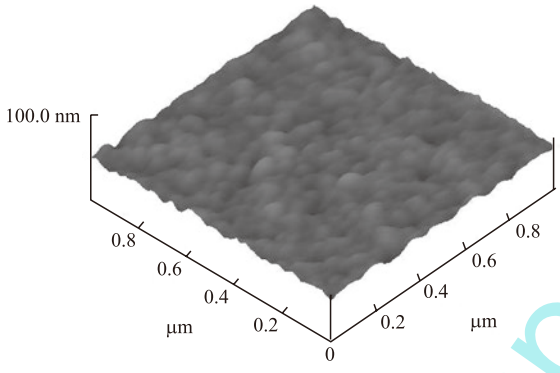

GZO RMS=3.6 nm
(b)

Fig.3 AFM images of the (a) AZO and (b) GZO thin films

Table 1 Electrical properties of the AZO and GZO thin films

Film	Resistivity/ ($\times 10^{-4}$ Ω cm)	Carrier concentration /($\times 10^{20}$ cm^{-3})	Hall mobility /(cm^2/V s)
AZO	10.1	6.5	9.5
GZO	3.5	14.6	12.3

Table 1 shows the electrical properties of the AZO and GZO thin films deposited on glass substrates at room temperature. The GZO thin film revealed an improved conductivity comparing with the AZO thin film: the resistivity decreased from 1.01×10^{-3} to 3.5×10^{-4} Ω cm, which was mostly due to the increase of the carrier concentration from 6.5×10^{20} to 1.46×10^{21} cm^{-3}. The increase of free carrier concentration was partially related to the increase of oxygen vacancies, as shown in Fig.2. On the other hand, because oxygen vacancy was a deep donor and there were few stable oxygen vacancies in ZnO[22], the free carrier concentration as high as10^{20}-10^{21} in the AZO or GZO films was a result of the donor electron from the Al or Ga dopant[17,22-24]. Thus, compared with the AZO film, the higher free carrier concentration for the GZO film could be mainly attributed to the much more Ga^{3+} ions at substitutional Zn^{2+} sites or interstitial positions, which acted as shallow donor. This indicated that the activation efficiency of Ga dopants could be much higher than that of Al dopants at the same doping level. In addition, the improvement of the mobility for the GZO thin film compared to the AZO thin film can be attributed to the improvement of the crystallinity, which was supported by the analysis of XRD. As described above, the GZO thin film had much higher peak value of XRD and much narrower value of FWHM than the AZO thin film, that is, it had the better crystal quality than the AZO thin film.

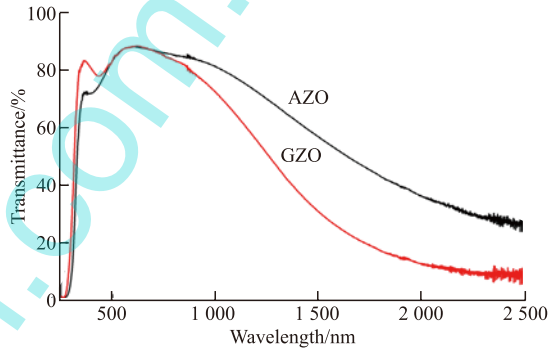

Fig.4 Optical transmittance of the AZO and GZO thin films

Fig.4 shows the optical transmission spectra of the AZO and GZO thin films deposited on glass substrates at room temperature. Both films showed average transmittance higher than 85% throughout the visible range. Compared to the AZO thin film, a drastic decrease in the transmittance in the infrared range was observed for the GZO thin film. This was caused by the free carrier absorption. On the other hand, the fundamental absorption edge of GZO thin film moved to the short wavelength region compared with that of AZO thin film, which was also attributed to the increase in the carrier concentration. The band gap widening with increasing carrier concentration was due to the filling of the conduction band by electrons, which was known as the Burstein-Moss effect[25,26].

4 Conclusions

AZO and GZO thin films with the same doping concentration were deposited on glass substrates by DC magnetron sputtering at room temperature. The GZO thin film presented a smoother surface morphology and better crystal quality than the AZO

thin film. The conductivity of the GZO thin film was improved compared to that of the AZO thin film: the resistivity decreased from 1.01×10^{-3} to 3.5×10^{-4} Ω cm, which was mostly due to the increase of the carrier concentration from 6.5×10^{20} to 1.46×10^{21} cm^{-3}. The increase of carrier concentration could be attributed to the much higher doping efficiency of Ga dopants in comparison with that of Al dopants and the increase of the concentration of oxygen vacancies. These results showed that the GZO thin film prepared at room temperature had better structural, morphological and electrical properties than that of the AZO thin film for optoelectronic applications.

References

[1] Kim J P, Bae J S, Hong T E, *et al.* Optical and Electrical Properties of ZnO Films, Codoped with Al and Ga Deposited at Room Temperature by an RF Sputtering Method[J].*Thin Solid Films*, 2010, 518: 6 179-6 183

[2] He L, Li Z, Zhang Z. Rapid, Low-Temperature Synthesis of Single-Crystalline Co_3O_4 Nanorods on Silicon Substrates on a Large Scale[J]. *Nanotechnology*, 2008, 19: 155 606

[3] Zhang D H, Yang T L, Ma J, *et al.* Preparation of Transparent Conducting ZnO:Al Films on Polymer Substrates by R. F. Magnetron Sputtering[J]. *Appl. Surf. Sci.*, 2000, 158: 43-48

[4] Wang X, Zeng X, Huang D, *et al.* The Properties of Al Doped ZnO Thin Films Deposited on Various Substrate Materials by RF Magnetron Sputtering[J]. *J. Mater. Sci. Mater. Electron*., 2012, 23: 1 580-1 586

[5] Anura P S, Luís M F R, Vitor G, *et al.* Cohesive Strength of Nanocrystalline ZnO:Ga Thin Films Deposited at Room Temperature[J]. *Nanoscale. Res. Lett*., 2011, 6: 309

[6] Elmas S, Korkmaz S. Deposition of Al Doped ZnO Thin Films on the Different Substrates with Radio Frequency Magnetron Sputtering[J]. *J. Non-Cryst. Solids*, 2013, 359: 69-72

[7] Tian J, Zhang Q, Uchaker E, *et al.* SnO-Nanocluster Modified Anatase TiO_2 Photocatalyst: Exploiting the Sn(II) Lone Pair for a New Photocatalyst Material with Visible Light Absorption and Charge Carrier Separation[J]. *J. Mater. Chem. A*, 2013, 1: 6 770-6 677

[8] Wang Z A, Chu J B, Zhu H B, *et al.* Growth of ZnO:Al Films by RF Sputtering at Room Temperature for Solar Cell Applications[J]. *Solid-State. Electron*., 2009, 53: 1 149-1 153

[9] Jin C G, Yu T, Wu Z F, *et al.* Room-Temperature Deposition of Transparent Conductive Al-doped ZnO Thin Films Using Low Energy Ion Bombardment[J]. *Appl. Phys. A*., 2012, 106: 961-966

[10] Mohanty B C, Yeon D H, Yun J H, *et al.* RF Power Dependence of Refractive Index of RoomTemperature Sputtered ZnO:Al Thin Films[J]. *Appl. Phys. A*, 2014, 115: 347-351

[11] Abduev A K, Akhmedov A K, Asvarov A S. The Structural and Electrical Properties of Ga-doped ZnO and Ga, B-codoped ZnO Thin Films: The Effects of Additional Boron Impurity[J]. *Sol. Energ. Mat. Sol. C*, 2007, 91: 258-260

[12] Kwak D J, Park M W, Sung Y M. Discharge Power Dependence of Structural and Electrical Properties of Al-doped ZnO Conducting Film by Magnetron Sputtering (for PDP)[J]. *Vacuum*, 2009, 83: 113-118

[13] Tao K, Sun Y, Cai H, *et al.* Deposition Ga-doped ZnO Films on PEN Substrate at Room Temperature for Thin Film Silicon Solar Cells[J]. *Appl. Surf. Sci*., 2012, 258: 5 943-5 946

[14] Pei Z L, Zhang X B, Zhang G P, *et al.* Transparent Conductive ZnO:Al Thin Films Deposited on Flexible Substrates Prepared by Direct Current Magnetron Sputtering[J]. *Thin Solid Films*, 2006, 497: 20-23

[15] Guillén C, Herrero J. Structure, Optical and Electrical Properties of Al:ZnO Thin Films Deposited by DC Sputtering at Room Temperature on Glass and Plastic Substrates[J]. *Phys. Status Solidi A*, 2009, 206: 1 531-1 536

[16] Lee B T, Kim T H, Jeong S H. Growth and Characterization of Single Crystalline Ga-doped ZnO Films Using RF Magnetron Sputtering[J]. *J. Phys. D: Appl. Phys*., 2006, 39: 957-961

[17] Jun M C, Park S U, Koh J H. Comparative Studies of Al-doped ZnO and Ga-doped ZnO Transparent Conducting Oxide Thin Films[J]. *Nanoscale. Res. Lett*., 2012, 7: 639

[18] Lennon C, Tapia R, Kodama R, *et al.* Effects of Annealing in a Partially Reducing Atmosphere on Sputtered Al-doped ZnO Thin Films[J]. *J. Electron. Mater*., 2009, 38: 1 568-1 573

[19] Zhu K, Yang Y, Wei T F, *et al.* Effects of Post-rapid Thermal Annealing on Structural, Electrical and Optical Properties of Hydrogenated Aluminum Doped Zinc Oxide Thin Films[J]. *J. Mater. Sci: Mater. Electron*., 2013, 24: 3 844-3 849

[20] Kim J M, Thiyagarajan P, Rhee S W. Direct Growth of Large Grain Polycrystalline Silicon Films on Aluminum-induced Crystallization Seed Layer Using Hot-Wire Chemical Vapor Deposition[J]. *Thin Solid Films*, 2010, 518: 5 860-5 865

[21] Zhu K, Yang Y, Wei T F, *et al.* Room Temperature DC Magnetron Sputtering Deposition of Hydrogenated Aluminum Doped Zinc Oxide Thin Films on Polyethylene Terephthalate Substrates[J]. *Mater. Lett*., 2013, 106: 363-365

[22] Jullien M, Horwat D, Manzeh F, *et al.* Influence of the Nanoscale Structural Features on the Properties and Electronic Structure of Al-doped ZnO Thin Films: an X-ray Absorption Study[J]. *Sol. Energ. Mat. Sol. C*, 2011, 95: 2 341-2 346

[23] Fang G, Lia D, Yao B L. Fabrication and Vacuum Annealing of Transparent Conductive AZO Thin Films Prepared by DC Magnetron Sputtering[J]. *Vacuum*, 2003, 68: 363-372

[24] Yue H, Wu A, Feng Y, *et al.* Structures and Properties of the Al-doped ZnO Thin Films Prepared by Radio Frequency Magnetron Sputtering[J]. *Thin Solid Films*, 2011, 519: 5 577-5 581

[25] Burstein E. Anomalous Optical Absorption Limit in InSb[J]. *Phys. Rev.*, 1954, 93: 632-633

[26] Moss T S. The Interpretation of the Properties of Indium Antimonide[J]. *Proc. Phys. Soc. B*, 1954, 67: 775